Arabian Journal of Chemistry (2023) **16**, 104879

King Saud University

Arabian Journal of Chemistry

www.ksu.edu.sa
www.sciencedirect.com

ORIGINAL ARTICLE

Metal ion/metal hydroxide loaded resin for ammonia removal from solutions containing high salinity by ligand exchange: Stability of metal ions during decomplexation of ammonia ligand

Chen Liu, Tingsheng Qiu, Yunnen Chen *

Jiangxi Key Laboratory of Mining & Metallurgy Environmental Pollution Control, Jiangxi University of Science & Technology, Ganzhou 341000, PR China

Received 20 November 2022; accepted 29 March 2023
Available online 14 April 2023

KEYWORDS

Ammonia;
High salinity;
Stability;
Metal-loaded resin;
Adsorption capacity;
Modification

Abstract Ligand exchange of ammonia with ammine-complexing transition metals loaded on the substrate has received more attention for removing ammonia from solutions containing high salinity. However, the stability between transition metal and substrate was destroyed by the desorbent in the process of the ligand exchanger recycling and ammonia ligand decomplexation, leading to metal elution and reducing the adsorption competency of the ligand exchanger. Herein, metal(ion)-loaded resins (Me(ion)-LR) were prepared and the stability of metal ions during the three-round ammonia adsorption–desorption process was studied. The results showed the ammonia adsorption capacity of Cu^{2+}-D751, Cu^{2+}/Ni^{2+}-D751 and Cu^{2+}/Zn^{2+}-D751 resin were 5.39, 5.80 and 5.65 mg/g, respectively and the shedding percent of Cu^{2+} is lower than that of Ni^{2+} and Zn^{2+}. Aimed for the high ammonia selectivity and low metal ion dissolution, metal(ion)-loaded resins were modified with NaOH to obtain metal(hydroxides)-loaded resins (Me(hydroxides)-LR). The stability of metal ions during the three-round ammonia adsorption–desorption process was also investigated. Meanwhile, the mechanism of the Me(hydroxides)-LR for ammonia removal was explored. The results suggested that the $Cu(OH)_x$-D751, $Cu(OH)_x$/$Ni(OH)_x$-D751 and $Cu(OH)_x$/$Zn(OH)_x$-D751 resin have higher ammonia adsorption capacity and reached 5.79, 8.25 and 7.94 mg/g, respectively. The shedding percent of Cu^{2+} and Zn^{2+} decreased obviously. Experimental and characterization

* Corresponding author.
E-mail address: cyn70yellow@126.com (Y. Chen).
Peer review under responsibility of King Saud University.

Production and hosting by Elsevier

https://doi.org/10.1016/j.arabjc.2023.104879

results show that the ammonia removal by Me(hydroxides)-LR was primarily due to coordination complexation and electrostatic interaction.

1. Introduction

Ammonia is considered as the most commonly occurring nitrogenous pollutant in wastewater and is widely derived from municipal and industrial sources (Koon et al, 1975; Fu et al, 2012; Atkins Jr et al, 2013). Ammonia concentration in water is an important indicator of the water quality, and the permitted level of ammonia in drinking water in China and European Union is set at 0.5 mg/L (Qin et al, 2011). Due to the potential drawbacks of ammonia release in the river basins that could cause eutrophication, harm aquatic ecosystems and human health (Zhang et al, 2018), the removal of ammonia from wastewater is thus mandatory.

In some cases, salinity commonly coexists in ammonia-rich wastewater (Wang et al, 2016), and high salinity means that the total salt mass fraction (calculated by NaCl) is not less than 1% (Lefebvre and Moletta, 2006). Although currently the main treatment technology for ammonia from water is biological process, it is inefficient to remove ammonia from high salinity wastewater because the high salinity inhibits biological activity by inducing cell plasmolysis due to rapid increase in osmotic pressure (Liu et al, 2014; Li et al, 2018). Therefore, many great efforts and techniques including ion exchange (Leyva-Ramos et al, 2010; Huang et al, 2010; Al-Sheikh et al., 2021), struvite precipitation (Zhu et al, 2016; Rahman et al, 2014), reverse osmosis (Keyikogluab et al, 2021) and electrochemical oxidation methods (Lahav et al, 2015) have been explored to remove ammonia from water containing high salinity. Among these listed technologies certainly, ion exchange method has received considerable attention for the treatment of ammonia in water due to its simple and effective process, high efficiency, and easy recycling of the exchange substrate (Mohd et al, 2019). However, the performance of exchangers is weakened by the salt environment with high concentrations of other common cations (e.g., Na^+, K^+, Mg^{2+}, Ca^{2+}) in wastewater, resulting in the decline of effluent quality (Berrin, 2012; Epsztein, 2019). This is because the selectivity of ion-exchange materials is dictated by differences in ion valence, hydration radius, and hydration energy (Huang et al, 2018). Generally, a large hydration radii and high energies lead to poor affinity for ion exchange functional groups, while a high valence leads to high affinity. Compared to ammonia in the solution, its hydration radius and hydration energy were roughly equal to K^+ but smaller than Na^+, and the divalent cations (Mg^{2+}, Ca^{2+}) exhibit higher affinity. When ammonia wastewater contains these high concentrations of competitive cations, the exchange rate of exchangers for ammonia drops significantly. Therefore, there is a need for high-capacity, environmentally-friendly, ammonia-selective adsorbents that can be easily and economically synthesized to achieve ammonia removal from wastewaters containing high salinity.

To improve the selectivity of the ion exchanger towards ammonia, the first report ammonia-selective ligand exchange was in 1962 by Helfferich in which ammonia was adsorbed to carboxylic acid cation-exchange resin Amberlite IRC-50 loaded with Cu^{2+}, Ni^{2+}, Zn^{2+}, Ag^+, Co^{3+}, and Fe^{3+} through the formation of complexes with the metal ions (“ligand sorption”) or through the displacement of other ligands that have previously complexed the metal (“ligand exchange”)(Helfferich, 1962). Typical “ligand exchange” reaction can be described in **Eq. (1)**.

$$\overline{R-Cu(H_2O)_4^{2+}} + 4NH_3 \rightleftharpoons \overline{R-Cu(NH_3)_4^{2+}} + 4H_2O \qquad (1)$$

Based on this concept, more attention has been paid to the application of metal-loaded adsorbents in the removal ammonia from water. Clark and Tarpeh (2020) prepared metal(ion)-loaded polymer ligand exchange resins by loading Zn, Cu on carboxylate resin (WAGG) and sodium iminodiacetate resin (SIR) individually to removal ammonia from wastewater containing other cations (Na^+, K^+, Ca^{2+}, Mg^{2+}), and found that metal ion binds to polymer ligand exchange resins via electrostatic attraction and complexation, while ammonia binds to the metal ions through ligand exchange with metal-aqua ligands. The presence of divalent cation (Ca^{2+}, Mg^{2+}) severely reduced ammonia adsorption and increased metal elution because of its stronger affinities to carboxylate/iminodiacetate resin and non-negligible ion exchange with transition metals. Mahata et al (2021) prepared Cu-loaded amino-functionalized SiO_2 and weak-base-anion-exchange resin containing primary and secondary amino groups, respectively for NH_4^+ removal. The results showed that a high NH_4^+ adsorption capacity was obtained and the adsorption of NH_4^+ went through endothermic deprotonation followed by exothermic complexation. Meanwhile, coexistence of high concentration (above 5.0 mM) of chloride-based salts (NaCl, KCl, $CaCl_2$, $MgCl_2$) inhibited the NH_4^+ adsorption and caused partial metal dissolution. Although Cl^- reduced positive charge on the resin surface, high ionic strength drove cations from the salts to replace the protons of NH_4^+ and combine with NH_3 to form ion pairs, thus suppressing the interaction between the NH_4^+ and the loaded Cu^{2+} ions (Jiang et al, 2010; El-Bayaa et al, 2009). The ability of the salts on the inhibition was in the order of $MgCl_2$ > $CaCl_2$ > KCl > NaCl (Mahata et al, 2021). Zhou et al (2015) investigated the adsorption capacity of Cu^{2+}-loaded chelating resin for ammonia in the adsorption–desorption process. It was found that the desorption percent of ammonia reached 93% under the conditions of 0.75 mol/L HCl as the desorption agent, desorption time 80 min and the circulating flow rate 12 L/h. In addition, Cu^{2+} content was detected in the desorption solution and the Cu^{2+} shedding percent increased with the increasing of HCl content. Wu (2017) prepared four kinds of metal-loaded resins through loading transition metal ions (Cu^{2+}, Co^{2+}, Ni^{2+}, Zn^{2+}) on the macro-porous weakly acidic cation exchange resin (D113) respectively. The comparison results indicated that the copper-loaded resin had the best ammonia adsorption capacity, reaching 6.49 mg/g, but the problem of metal ions falling off existed in desorption and regeneration process. According to the above researches, although the prepared metal-loaded adsorbent certainly achieved high selectivity and adsorption capacity for ammonia, there is still a common problem, that is, metal ions are prone to dissolve from the adsorbent into the solution during the adsorption–desorption process, causing metal pollution and reducing the adsorption performance of the adsorbent for ammonia. Therefore, how to ensure a high ammonia desorption percent while avoiding the desorption of metal ions is necessary.

In this paper, metal(ion)-loaded resins (named Me(ion)-LR) were prepared through loading metal ions (Cu^{2+}, Zn^{2+}, Ni^{2+}) as the active species on a cation exchange resin chelating amine-carboxyl-group (D751). The stability of metal ions on the Me(ion)-LR for ammonia removal from water containing high salinity during adsorption–desorption process was studied. On this basic, aim for the high ammonia selectivity and low metal ion dissolution, metal(hydroxides)-loaded resins (named Me(hydroxides)-LR) were prepared through impregnation the Me(ion)-LR in NaOH solution. The adsorption capacity of the Me(hydroxides)-LR for ammonia removal from solution contain-

ing high salinity under different NaOH concentration and modification time were determined. The stability of metal ions on the Me (hydroxides)-LR during adsorption–desorption process was also investigated. Meanwhile, the interactions among the resin, metal ion, and ammonia were explicitly characterized with scanning electron microscope (SEM), N_2 adsorption–desorption analysis, infrared spectroscopic (FTIR) and X-ray photoelectron spectroscopy (XPS). In addition, the mechanism of the Me(hydroxides)-LR for ammonia removal has been discussed with respect to different desorbents, NaCl concentration and desorption time.

2. Experimental

2.1. Materials

The virgin macro-porous chelated styrene ion exchange resin D751 containing iminodiacetic acid as ligand used in this study was taken from Shanghai Macklin Biochemical Co., Ltd., China. Its properties as reported by the suppliers are listed in **Table S1**.

Copper nitrate trihydrate ($Cu(NO_3)_2{\cdot}3H_2O$), zinc nitrate hexahydrate ($Zn(NO_3)_2{\cdot}6H_2O$), nickel nitrate hexahydrate ($Ni(NO_3)_2{\cdot}6H_2O$), ammonium chloride (NH_4Cl), sodium chloride (NaCl), sodium hydroxide (NaOH) and hydrochloric acid (HCl, 36%) were received from Shanghai Sinopharm Chemical Reagent Co., Ltd., China. All the chemicals were analytical reagents, and deionized water with a resistivity of 18.2 MΩ·cm was prepared by a water purification system (TE-S20, Hitech Instruments Co., Ltd, China) for the preparation of all aqueous solutions.

2.2. Preparation and characterization of adsorbent

To remove non-adhesive impurities and small particles, the origin D751 resin was washed repeatedly with deionized water, and then dried in an oven at 323 K for 24 h. Subsequently, the Na-form modified D751 resin (Na^+-D751), which was used as the substrate for metal ion loading, was obtained using 1 mol/L NaOH and 1 mol/L HCl solution. The first step is to immerse the resin in 2 bed volume (BV) of NaOH for 4 h and then wash it with deionized water until the effluent is neutral. The second is to immerse the resin in 2 BV of HCl for 4 h and then wash it with deionized water until the effluent is neutral. The third is to immerse the resin in 4 BV of NaOH for 12 h, then wash it with deionized water until neutral, and by drying in an oven at 323 K for 24 h.

After that, the Na^+-D751 resins (1 g) were dispersed in 200 mL of $Cu(NO_3)_2$ solution (concentration of Cu^{2+} was 0.005 mol/L), $Cu(NO_3)_2/Zn(NO_3)_2$ solution (concentration of Cu^{2+} and Zn^{2+} were 0.05 mol/L) and $Cu(NO_3)_2/Ni(NO_3)_2$ solution (concentration of Cu^{2+} and Ni^{2+} were 0.05 mol/L) under stirring at 120 r/min for 90, 120 and 180 min, respectively. After adsorption equilibrium, the resin was collected by filtration and rinsed with deionized water for several times and then dried in an oven at 323 K for 5 h. The resulting Me (ion)-LR were called Cu^{2+}-D751, Cu^{2+}/Zn^{2+}-D751 and Cu^{2+}/Ni^{2+}-D751, respectively.

The Me(hydroxides)-LR were prepared using an impregnation method as follows: 1 g Me(ion)-LR (Cu^{2+}-D751, Cu^{2+}/Zn^{2+}-D751 and Cu^{2+}/Ni^{2+}-D751) was added into 100 mL of NaOH solution with the desired concentration (0, 0.001, 0.005, 0.0075, 0.01, 0.02 mol/L) and stirred at 120 r/min for a certain time (0, 5, 15, 30 and 45 min). Afterward, the resin was collected by filtration and rinsed with deionized water for several times and dried in an oven at 323 K for 300 min. The obtained samples were called $Cu(OH)_x$-D751, $Cu(OH)_x/Zn(OH)_x$-D751 and $Cu(OH)_x/Ni(OH)_x$-D751, respectively.

Surface morphological characterizations of the above-mentioned resins were analyzed by a scanning electron microscopy (SEM) analyzer (MLA650F, FEI, US) under an acceleration voltage of 15 kV. The microstructural characterization and chemical compositions of the resins were characterized with an X-ray photoelectron spectroscopy (XPS) spectrometer (ESCALAB 250, Thermo-VG Scientific, US) and a fourier-transformed infrared (FTIR) spectrometer (NEXUS 670, Nicolet, US). The specific surface areas, pore volume and pore diameter of the resins were determined from N_2 adsorption–desorption isotherm measurements at 77 K according to the Brunauer Emmett-Teller (BET) method, using an analyzer ASAP 2020 made by Micromeritics.

2.3. Adsorption experiments

The sorption of ammonia in water was performed in a 250 mL batch reactor with sealing plug at room temperature (298 ± 2 K). The adsorption experiment process is as follows. Firstly, a 1.0 g/L NH_3-N stock solution was prepared by dissolving 3.819 g NH_4Cl solid into 1000 mL deionized water, and then diluted to the desired initial concentration of 0.1 g/L. Secondly, the batch reactor was filled with 100 mL of 0.1 g/L NH_3-N solution and then alkalized to a set pH value of 11 with 1 mol/L NaOH. Thirdly, 0.4 g NaCl solid was introduced in the reactor and then fully dissolved. Subsequently, 0.6 g adsorbent was added to the reactor and then covered the sealing plug. Finally, the mixture was stirred in a SHA-C temperature-controlled water-bath oscillator at 120 r/min for 90 min.

In addition, a blank experiment, in the absence of any adsorbent, was carried out under the conditions of an initial ammonia solution pH of 11, dosage of NaCl 4 g/L, stirring speed 120 r/min and reaction time 90 min. After the reaction, the concentration of ammonia in the liquid samples was measured by Nessler's reagent spectrophotometry method (HJ 535–2009). The results show that ammonia adsorption capacity is less than 0.5 mg/g.

2.4. Desorption experiments

The spent adsorbent (0.4 g) was soaked in 100 mL 1 mol/L NaCl solution under shaking at 120 r/min for 60 min. Afterwards, the resin was collected by filtration, rinsed by deionized water, and dried at 323 K for 5 h for the next run of ammonia adsorption.

2.5. Analysis

After adsorption, the resin was recovered from the suspensions by filtration and the remaining concentration of ammonia in the liquid samples was measured by Nessler's reagent spectrophotometry method (HJ 535–2009). The adsorption capacity (Q, mg/g) of ammonia was calculated by **Eq. (2)**, where C_0 and C_1 are initial and residual concentration of ammonia (mg/L) in the liquid phase, respectively, V_0 is the volume of ammo-

nia solution (L) and m is the mass of adsorbent used (g). The metal-ions concentration in the liquid samples was quantified by Atomic absorption spectroscopy (AAS). The loading capacity (q, mg/g) of metal ions was calculated by **Eq. (3)**, where W_0 and W_1 are the concentration of metal ions in the metal salt solution before and after loading (mg/L), respectively, and V_1 is the volume of metal salt solution (L). The metal ions shedding percent (η, %) of the metal-loaded resin was calculated by **Eq. (4)**, where M is the concentration of metal ions in the liquid samples after reaction (mg/L), and V_2 is the volume of the liquid samples after reaction (L). All experiments were performed in triplicate, and only the mean values have been reported.

$$Q = \frac{(C_0 - C_1) \cdot V_0}{m} \tag{2}$$

$$q = \frac{(W_0 - W_1) \cdot V_1}{m} \tag{3}$$

$$\eta(\%) = \frac{M \cdot V_2}{m \cdot q} \times 100\% \tag{4}$$

The ammonia desorption percent R (%) was obtained according to **Eq. (5)**, where N is the ammonia concentration in the eluent after desorption (mg/L), N_0 is initial ammonia concentration in the liquid phase before adsorption (mg/L), and N_1 is residual ammonia concentration in the liquid phase after adsorption saturation (mg/L).

$$R(\%) = \frac{N}{N_0 - N_1} \times 100\% \tag{5}$$

3. Results and discussion

3.1. Ammonia removal by Me(ion)-LR

3.1.1. Reusability and stability of Me(ion)-LR

In this experiment, three resins (Cu^{2+}-D751, Cu^{2+}/Ni^{2+}-D751 and Cu^{2+}/Zn^{2+}-D751) were used to adsorb ammonia from solution containing high salinity. Subsequently, these spent resins were regenerated by 1 mol/L NaCl solution. Three runs of ammonia saturated Cu^{2+}-D751, Cu^{2+}/Ni^{2+}-D751 and Cu^{2+}/Zn^{2+}-D751 resins were performed and the shedding percent of metal-ions during the adsorption–desorption process were investigated. The corresponding results are shown in Fig. 1 and Table 1.

From Fig. 1, after three rounds of adsorption–desorption process, the ammonia adsorption capacity of Cu^{2+}-D751 resin decreased slightly and remained at roughly 81% of original value. However, the ammonia adsorption capacity of Cu^{2+}/Ni^{2+}-D751 and Cu^{2+}/Zn^{2+}-D751 resins at the second and third rounds were significantly higher than that of at the first round. Such an increment could be attributed to the conversion of Me(ion)-LR to Me(hydroxides)-LR after being desorbed by NaCl solution. For Me(ion)-LR, the ammonia adsorption mechanisms have been identified as the electrical interaction and coordination complexation. In an ammonia nitrogen solution under alkaline conditions, the metal adsorption sites on Me(ion)-LR absorbed portion of OH^- in water to make the resin surface showed electronegative, which was conducive to the adsorption of NH_4^+ in the form of ionic bonds through electrostatic interaction. On the other hand, the metal adsorption sites on Me(ion)-LR and N atom in NH_3 form a coordination bond by sharing the lone pair of electrons provided by N, O atom, thus forming a metal ammonia complex loaded resin. The Me(ion)-LR $\left(\overline{R-Me^{2+}}\right)$ becomes an ammonia-saturated resin $\left(\overline{R-Me(NH_3)_n(OH)_m}\right)$ after reaching equilibrium in ammonia adsorption process. When NaCl solution is used as a neutral salt for the desorption of ammonia-saturated resin, it plays a role in reducing the stability of, which promotes the shift of $\overline{R-Me(NH_3)_n(OH)_m}$ into $\overline{R-Me(OH)_m}$ and then NH_3 be eluted from the resin. Therefore, partial metal ion adsorption site on Me(ion)-LR have been converted to Me(hydroxides)-LR after the first desorption process. Comparing with Me(ion)-LR, Me(hydroxides)-LR has better ammonia bonding ability probably because of the inhibition of aeolotropic metal hydroxides that is formed

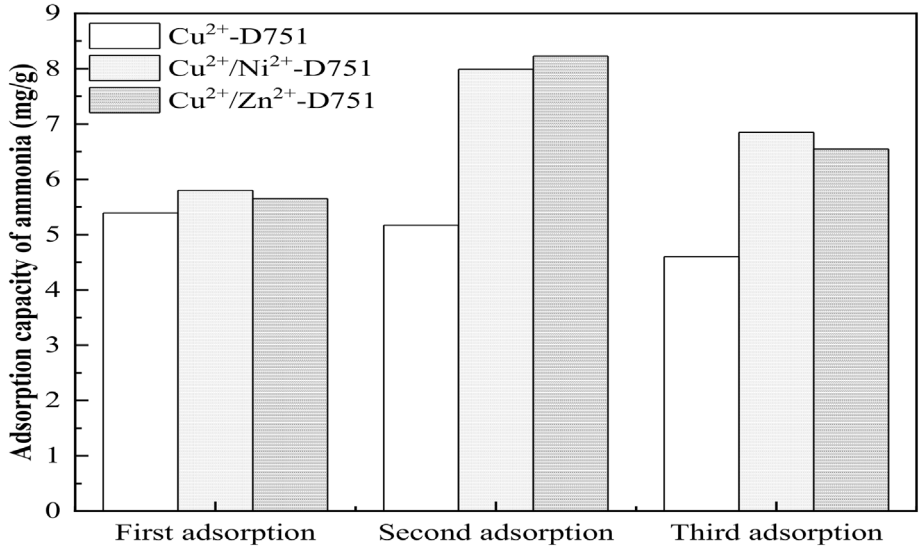

Fig. 1 The performance of ammonia removal for Cu^{2+}-D751, Cu^{2+}/Ni^{2+}-D751 and Cu^{2+}/Zn^{2+}-D751 resins.

Table 1 The loading capacity and shedding percent of metal-ions in the adsorption and desorption process for Me(ion)-LR.

	State of resin	Cu^{2+}-D751	Cu^{2+}/Ni^{2+}-D751		Cu^{2+}/Zn^{2+}-D751	
		Cu^{2+}	Cu^{2+}	Ni^{2+}	Cu^{2+}	Zn^{2+}
Loading capacity of metal ion	/	54.36 mg/g (0.85 mmol/g)	140.25 mg/g (2.19 mmol/g)	52.75 mg/g (0.90 mmol/g)	124 mg/g (1.94 mmol/g)	17.25 mg/g (0.27 mmol/g)
Shedding percent of metal ion (%)	1st adsorption	0.04	ND	0.17	0.02	0.64
	1st desorption	0.09	0.04	1.65	0.06	4.08
	2nd adsorption	ND	0.05	ND	ND	ND
	2nd desorption	0.09	0.04	1.29	0.04	0.18
	3rd adsorption	ND	0.03	ND	ND	ND
	3rd desorption	0.08	0.04	1.25	0.04	0.34

by the resin and the well-dispersed metal hydroxides (Dong et al, 2017).

Table 1 shows that the loading capacity of Cu^{2+} on Cu^{2+}-D751 resin was 54.36 mg/g, while the loading capacity of Cu^{2+} and Ni^{2+} on Cu^{2+}/Ni^{2+}-D751 resin and Cu^{2+} and Zn^{2+} on Cu^{2+}/Zn^{2+}-D751 resin were 140.25, 52.75 mg/g and 124, 17.25 mg/g, respectively. In conjunction with Fig. 1, it can be seen that the ammonia adsorption capacities of Cu^{2+}/Ni^{2+}-D751 (5.80 mg/g) and Cu^{2+}/Zn^{2+}-D751 (5.65 mg/g) in the first adsorption process were slightly higher than that of Cu^{2+}-D751 (5.39 mg/g), which is attributed to the bimetallic ion loaded resins have a higher metal loading, so it can provide more effective ammonia adsorption sites.

On the other hand, as shown in Table 1, the Cu^{2+} shedding percents in the three adsorption–desorption process of ammonia removal by Cu^{2+}-D751, Cu^{2+}/Ni^{2+}-D751 and Cu^{2+}/Zn^{2+}-D751 resin were detected not to exceed 0.09%. For Cu^{2+}/Ni^{2+}-D751 resin, the Ni^{2+} shedding percent was detected only in the first adsorption process and the Ni^{2+} shedding percent was 0.17%. Three-round desorption process in ammonia removal by Cu^{2+}/Ni^{2+}-D751 resin, the maximum Ni^{2+} shedding percent was 1.65%. For Cu^{2+}/Zn^{2+}-D751 resin, the Zn^{2+} shedding percent was detected only in the first adsorption process and the Zn^{2+} shedding percent was 0.64%. However, the maximum Zn^{2+} shedding percent reached 4.08%.

From the above results, it can be found that when using Me(ion)-LR to remove ammonia from water containing high salinity during the adsorption–desorption process, there is indeed a problem of metal ions dissolving from the Me(ion)-LR into the liquid phase. However, the shedding percent of Cu^{2+} is lower than that of Ni^{2+} and Zn^{2+}, because the stability order of the chelate formed by metal ion and iminodiacetate moieties on D751 resin is: $Cu^{2+} > Ni^{2+} > Zn^{2+}$ (Zhang et al, 1990).

3.1.2. Characterizations of Me(ion)-LR

The SEM images (a-j) of the Na^+-D751 resin (a), Me(ion)-LR (b ~ d), and Me(ion)-LR after first adsorption and desorption (e ~ j) are shown in Fig. 2. As indicated in Fig. 2 **(a)**, the Na^+-D751 resin clearly exhibits a skeleton structure connected by small particles. After metal(ion) loading, it contained film-like species coating on the resin skeleton structure, and the coating degree of the film-like species on the Cu^{2+}/Zn^{2+}-D751 resin (Fig. 2 **(d)**) was highest, followed by Cu^{2+}-D751 (Fig. 2 **(b)**) and Cu^{2+}/Ni^{2+}-D751 resin (Fig. 2 **(c)**). After ammonia adsorption, the film-like species was more evenly coated on the resin surface, as shown in Fig. 2 **(e)~(g)**. Meanwhile, compared to Me(ion)-LR (Fig. 2 **(b)~(d))**, the surface morphology of the Me(ion)-LR after first desorption (Fig. 2 **(h ~ j)**) changed insignificantly.

Fig. S1 shows that the N_2 adsorption and desorption isotherms of the seven resins exhibited typical type IV with H1 hysteresis loop according to IUPAC classification (Saha and Deng, 2010). The initial part of the type IV is attributed to monolayer–multilayer adsorption according to Nawrocki et al (1993). This H1 hysteresis loop probably arises from the agglomerates loading to narrow pore size distribution. The specific surface areas, pore volume and mean pore diameter of the Na^+-D751 resin, Me(ion)-LR after first adsorption and Me(ion)-LR after first desorption were summarized in Table 2. It can be seen that after metal ion loading, the specific surface area and pore volume of the resins were increased, while the mean pore diameter decreased. This changes in BET surface area and pore textural properties can be explained by the formation of bridge complex between metal ion and the iminodiacetate moieties. It was worth noting that the specific surface area of three Me(ion)-LR after the first adsorption decreased obviously, especially the latter two resin, from 18.2 to 14.8 m^2/g and 18.3 to 15.4 m^2/g, respectively, which could be interpreted by the formation of complex between ammonia and transition metals. Moreover, the BET surface areas, pore volume and mean pore diameter of Me(ion)-LR after first desorption were smaller than the Na^+-D751 resin, Me(ion)-LR after first adsorption, which further indicates that the properties of Me(ion)-LR after regeneration have changed.

FTIR analysis was used to provide evidence of comparable difference between the (a) Na^+-D751, (b) Cu^{2+}-D751, (c) Cu^{2+}/Ni^{2+}-D751(c) and (d) Cu^{2+}/Zn^{2+}-D751 resins (Fig. 3 (A)). The adsorption peak at 3457 cm^{-1} assigned to the –OH stretching vibration peak with respect to –COOH groups (Prabhu et al, 2014). After loading metal ion on D751, the

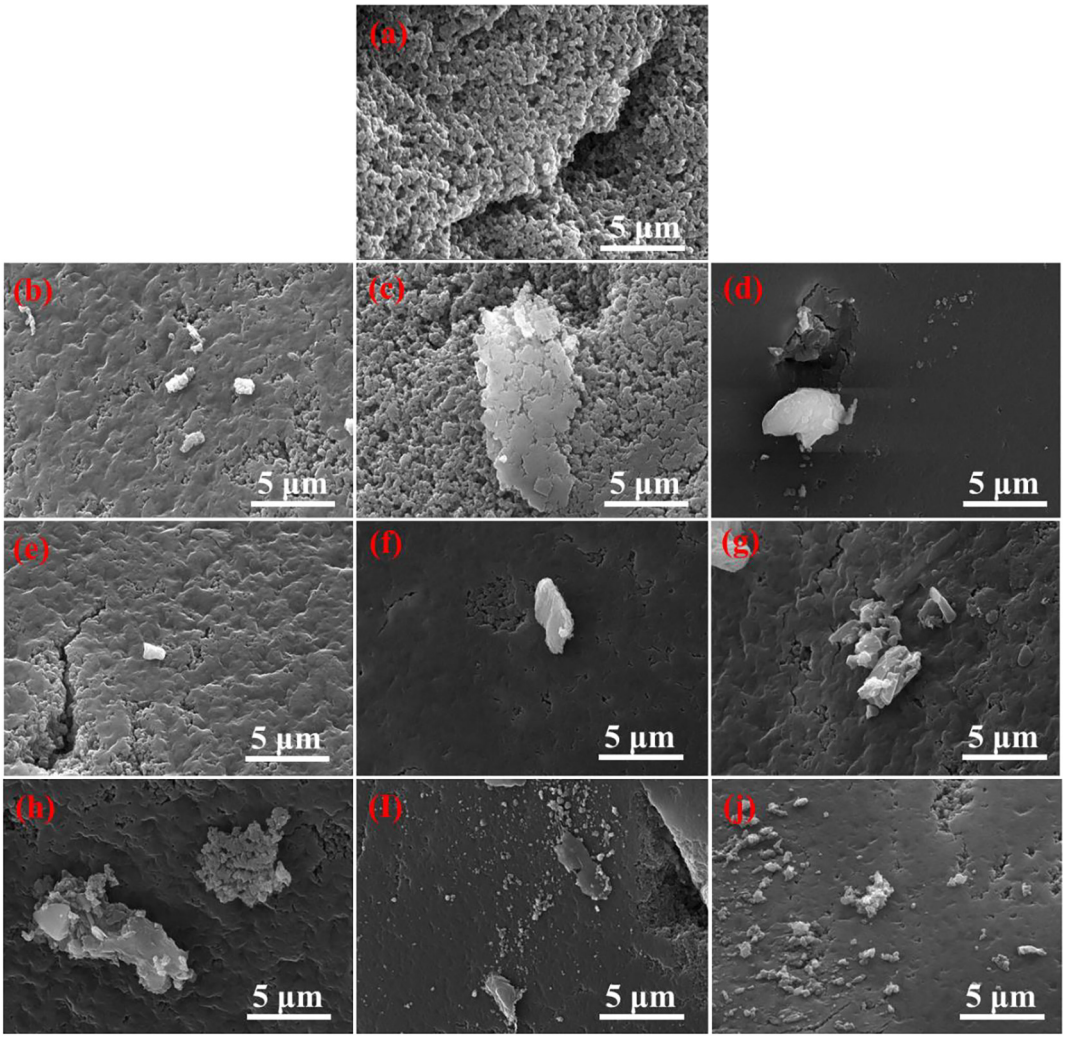

Fig. 2 SEM images of (a) Na^{+}-D751, (b) Cu^{2+}-D751, (c) Cu^{2+}/Ni^{2+}-D751, (d) Cu^{2+}/Zn^{2+}-D751, (e) Cu^{2+}-D751 after the first adsorption, (f) Cu^{2+}/Ni^{2+}-D751 after the first adsorption, (g) Cu^{2+}/Zn^{2+}-D751 after the first adsorption, (h) Cu^{2+}-D751 after the first desorption, (i) Cu^{2+}/Ni^{2+}-D751 after the first desorption, (j) Cu^{2+}/Zn^{2+}-D751 after the first desorption.

Table 2 N_2 adsorption–desorption analysis data of Me(ion)-LR.

Different types of Me(ion)-LR	State of Me(ion)-LR	Surface area (m^2/g)	Pore volume (cm^3/g)	Mean pore diameter (nm)
D751 resin	Unused	10.7	0.012	4.51
Cu^{2+}-D751 resin	Unused	12.5	0.014	4.40
	After first adsorption	12.4	0.014	4.41
	After first desorption	12.4	0.014	4.42
Cu^{2+}/Ni^{2+}-D751 resin	Unused	18.2	0.020	4.46
	After first adsorption	14.8	0.016	4.30
	After first desorption	14.6	0.016	4.32
Cu^{2+}/Zn^{2+}-D751 resin	Unused	18.3	0.020	4.45
	After first adsorption	15.4	0.017	4.37
	After first desorption	14.8	0.016	4.36

intensity of peak was obviously weakened and shifted to 3453, 3468, 3475 cm^{-1}. It might be that the forming of coordination bond between the O atom on the –OH and metal ion, as shown in **Fig. S2** (Chen et al, 2017). The peaks appeared 3025, 2924 and 2849 cm^{-1} belonged to the C–H stretching vibrations of saturated alkyl groups (Yuan et al, 2006). After loading metal ion, the peaks were changed insignificantly, probably because saturated alkyl groups were not participated in the adsorption reaction. The absorption peak at 1630 cm^{-1} and 1402 cm^{-1} attributed the vibration absorption peak about the carboxylate

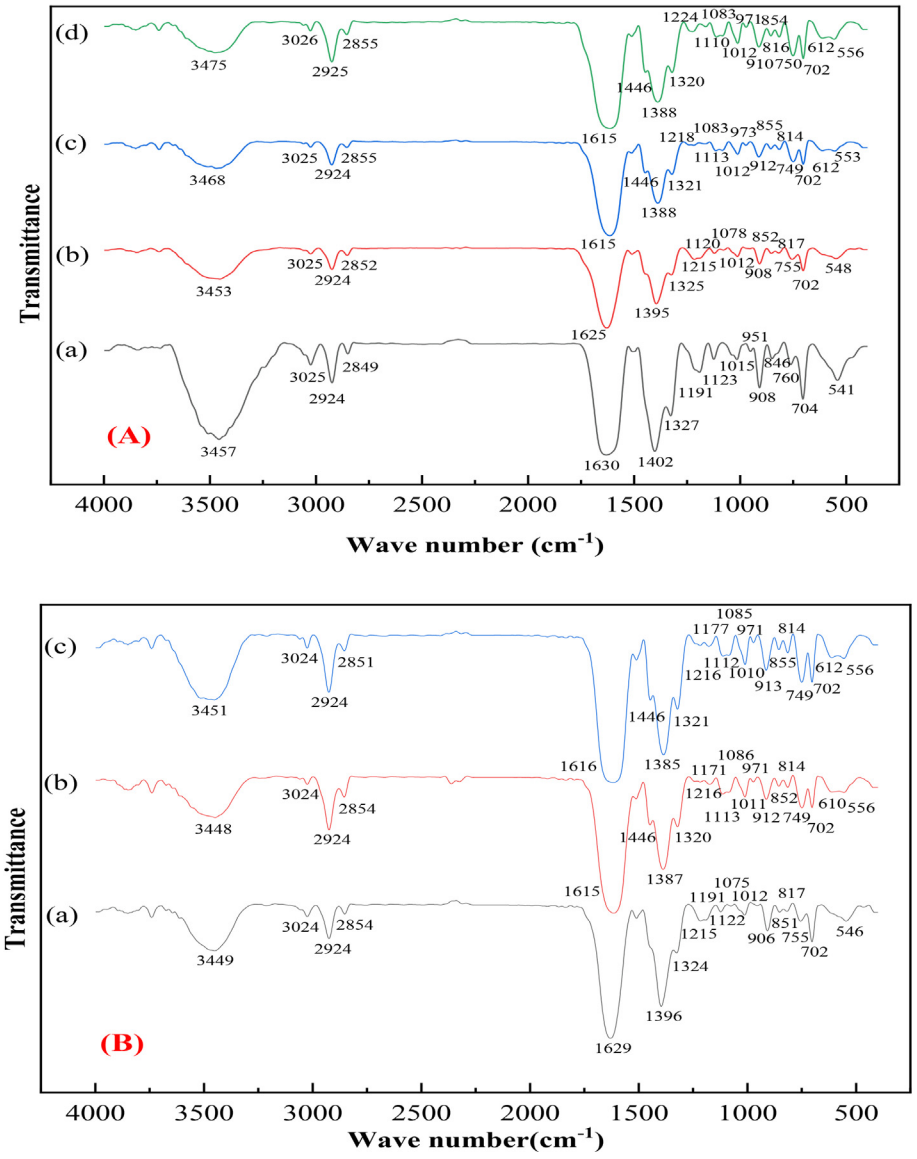

Fig. 3 FTIR spectra of (A) Me(ion)-LR ((a) Na^+-D751, (b) Cu^{2+}-D751, (c) Cu^{2+}/Ni^{2+}-D751 and (d) Cu^{2+}/Zn^{2+}-D751), (B) Me (hydroxides)-LR ((a) $Cu(OH)_x$-D751, (b) $Cu(OH)_x$/$Ni(OH)_x$-D751, (c) $Cu(OH)_x$/$Zn(OH)_x$-D751).

on iminodiacetate moieties (Prabhu et al, 2014), and the peaks after loading metal ion were also shifted to 1625, 1615 cm^{-1} and 1395, 1388 cm^{-1}, respectively. It could be classified to the formation of a coordination bond between metal ion and O from carboxylate on iminodiacetate moieties, as shown in **Fig. S2** (Chen et al, 2017; Zhang et al, 2020). In addition, the C-N peak at 1191 cm^{-1} was shifted to 1215, 1218 and 1224 cm^{-1} may be due to the binding of metal ion to N-donor atom for iminodiacetate-type exchangers. (Igberase et al, 2017; Sengupta et al, 1991).

3.2. Ammonia removal by Me(hydroxides)-LR

In order to solve the problem of metal ions shedding in adsorption and desorption process, three kinds of Me(ion)-LR were modified by NaOH solution to obtain $Cu(OH)_x$-D751, $Cu(OH)_x$/$Ni(OH)_x$-D751 and $Cu(OH)_x$/$Zn(OH)_x$-D751 resin. The effects of Me(hydroxides)-LR prepared under different NaOH concentrations and modification time on the treatment of ammonia solution containing high salinity and the stability of Me(hydroxides)-LR were also investigated.

3.2.1. Effect of NaOH concentration

Fig. 4 **(a)** shows the effect of Me(hydroxides)-LR prepared under different NaOH concentrations (from 0 to 0.02 mol/L) on ammonia removal. It can be seen from Fig. 4 **(a)** that the adsorption capacity of $Cu(OH)_x$-D751 resin for ammonia increased firstly and then decreased with the increasing of NaOH concentration, and reached maximum at 0.005 mol/L. The results can be interpreted as follow: initially, the partial of metal adsorption sites on Me(ion)-LR absorbed OH^- to form Me(hydroxides)-LR $\overline{(R-Cu(OH)_x)}$, which makes the resin surface showed electronegative, thus facilitating the adsorption of NH_4^+ in the form of ionic bonds through electrostatic interaction. Meanwhile, the other partial of metal adsorption sites on Me(ion)-LR absorbed NH_3 in the form

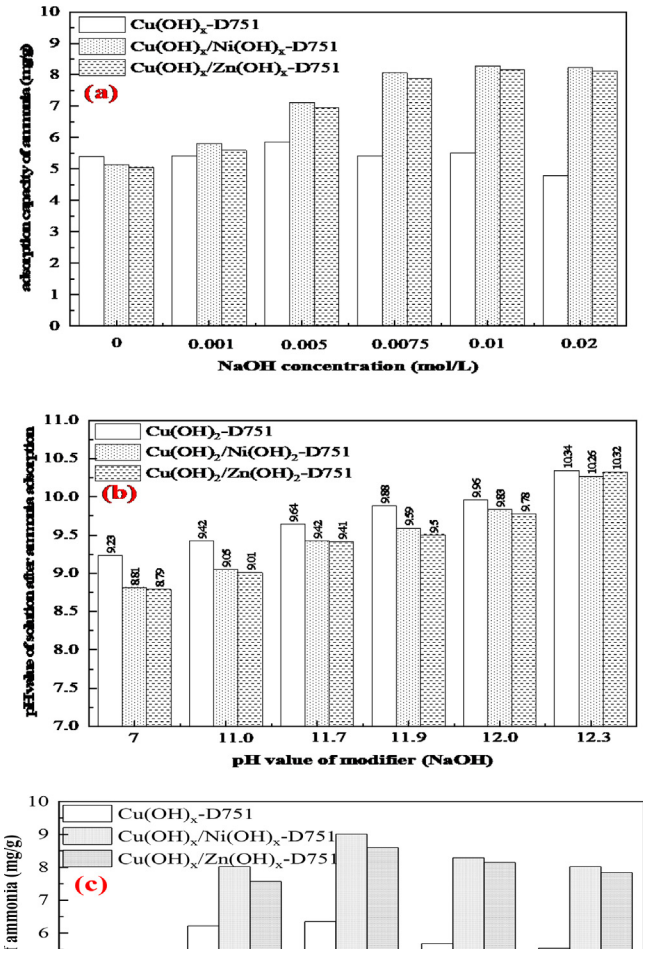

Fig. 4 Effect of (a) NaOH concentration and (b) changes of pH value of solution after ammonia adsorption by Me(hydroxides)-LR, (c) modification time on ammonia removal by Me(hydroxides)-LR.

of coordination bond through coordination complexation to form copper ammonia complex. When the NaOH concentration was 0.005 mol/L, the synergistic effect of electrostatic interaction and coordination complexation on ammonia adsorption reaches the maximum. Further increasing the concentration of NaOH, the metal adsorption sites on Me(ion)-LR were more occupied by OH^-. The adsorption capacity of $Cu(OH)_x$/$Ni(OH)_x$-D751 and $Cu(OH)_x$/$Zn(OH)_x$-D751 resin for ammonia increased with the increasing in NaOH concentration, and attained maximum at 0.01 mol/L. Compared with $Cu(OH)_x$-D751 resin, bimetallic hydroxide loaded resin has a higher metal loading, so it can provide more effective ammonia adsorption sites. Fig. 4 **(b)** exhibits the changes of pH value of reaction solution after ammonia adsorption by Me(hydroxides)-LR prepared under different NaOH concentrations (the corresponding pH value of modifier at each concentration from 7 to 12.3) on ammonia removal. The results suggested that the pH values of solution after ammonia adsorption by either Me(ion)-LR or Me(hydroxides)-LR were lower than that of the initial solution (pH = 11). On the one hand, when the pH of the initial solution was 11, most of ammonia was presented as molecular NH_3(aq) (**Eq. (6)**) (Yu et al., 2021; Chen et al., 2018). The coordination complexation between NH_3(aq) and metal adsorption sites on the resin were carried out continuously, which reduced the content of NH_3(aq) in the solution, promoted the proportion of NH_3(aq)/NH_4^+(aq) to shift towards NH_3(aq), thus leading to the decrease of the pH value of the solution.

$$NH_4^+ + OH^- \rightleftharpoons NH_3(aq) + H_2O \quad (6)$$

On the other hand, it can also be found from Fig. 4(b) that the adsorption of ammonia by Me(hydroxides)-LR would also provide OH^- and promoted the conversion of NH_4^+(aq) to NH_3(aq), resulting in a further increase in ammonia removal. Consequently, the change in solution pH values should be a trade-off between above two effects.

3.2.2. Effect of modification time

Fig. 4(c) shows that the influence of Me(hydroxides)-LR obtained by varying modification time on ammonia removal. The adsorption capacity of $Cu(OH)_x$-D751, $Cu(OH)_x$/$Ni(OH)_x$-D751 and $Cu(OH)_x$/$Zn(OH)_x$-D751 resin for ammonia in solution increased firstly and then decreased with the increasing of modification time, and reached maximum when the modification time was 15 min. One reasonable explanation is that a combination of OH^- and metal ions on Me(ion)-LR formed metal hydroxide in a relatively short time. The existing form of the loaded metal ion on resin changed, which was conducive to the adsorption of ammonia. With the extension of NaOH treatment time, the metal ions on Me(ion)-LR fell off, resulting in the decrease of the ammonia adsorption performance.

3.2.3. Reusability and stability of Me(hydroxides)-LR

In this experiment, three resins ($Cu(OH)_x$-D751, $Cu(OH)_x$/$Ni(OH)_x$-D751 and $Cu(OH)_x$/$Zn(OH)_x$-D751 resin) were used to adsorb ammonia. Subsequently, these spent resins were desorbed using 1 mol/L NaCl solution and used to treat ammonia again. Three successive desorption and regeneration processes were carried out. The performance of ammonia removal for Me(hydroxides)-LR and the shedding percent of metal ions during the adsorption and desorption process were investigated. The results are shown in Fig. 5 and Table 3, respectively.

Fig. 5 indicates that the adsorption capacity of three resins for ammonia decreased gradually after three times of desorp-

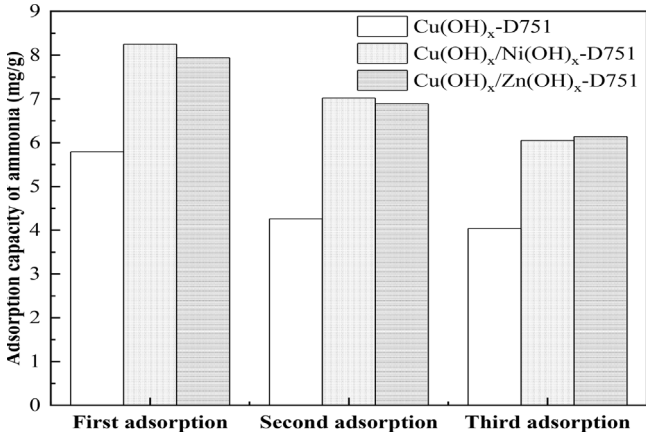

Fig. 5 The adsorption capacity of $Cu(OH)_x$-D751, $Cu(OH)_x$/$Ni(OH)_x$-D751, $Cu(OH)_x$/$Zn(OH)_x$-D751 resin for ammonia after three times of adsorption–desorption process.

Table 3 The Me(hydroxides)-LR loading capacity and shedding percent of metal-ions during adsorption–desorption process.

	State of resin	$Cu(OH)_x$-D751	$Cu(OH)_x/Ni(OH)_x$-D751		$Cu(OH)_x/Zn(OH)_x$-D751	
		Cu^{2+}	Cu^{2+}	Ni^{2+}	Cu^{2+}	Zn^{2+}
Loading capacity of metal ion	/	54.36 mg/g (0.85 mmol/g)	140.16 mg/g (2.19 mmol/g)	52.51 mg/g (0.89 mmol/g)	123.92 mg/g (1.94 mmol/g)	16.98 mg/g (0.26 mmol/g)
Shedding percent of metal ion (%)	1st adsorption	0.05	0.02	0.30	ND	ND
	1st desorption	0.06	0.03	4.81	0.02	0.71
	2nd adsorption	ND	0.08	0.28	0.02	0.24
	2nd desorption	0.06	0.03	3.82	0.03	0.24
	3rd adsorption	ND	0.05	0.36	0.02	0.24
	3rd desorption	0.05	0.02	3.44	0.02	0.24

ND: the concentration of metal ions in solution was not detected by the atomic absorption spectroscopy.

tion and regeneration. The third adsorption capacity of $Cu(OH)_x$-D751, $Cu(OH)_x/Ni(OH)_x$-D751 and $Cu(OH)_x/Zn(OH)_x$-D751 resin for ammonia were 4.04 mg/g, 6.05 mg/g and 6.14 mg/g, respectively, which remained at 70%, 73% and 77% of the first adsorption capacity, respectively.

Compared with Me(ion)-LR (Table 1), the loading capacity of metal ions on the Me(hydroxides)-LR (Table 3) were not changed obviously. In addition, it can be observed from Table 3 that for $Cu(OH)_x$-D751 resin, the leakage of Cu^{2+} was detected only in the first adsorption process and the Cu^{2+} shedding percent was 0.05%. The Cu^{2+} shedding percent in three desorption processes were lower than that of in the Cu^{2+}-D751 resin. In addition, compared with Cu^{2+}/Zn^{2+}-D751 resin, the Zn^{2+} shedding percent of $Cu(OH)_x/Zn(OH)_x$-D751 resin in first desorption process was significantly reduced from 4.08% to 0.71%. However, the Ni^{2+} shedding percent of $Cu(OH)_x/Ni(OH)_x$-D751 resin in three adsorption and desorption processes were higher than that of Cu^{2+}/Ni^{2+}-D751 resin.

3.2.4. Characterizations of Me(hydroxides)-LR

Fig. 6 presents SEM micrographs of Me(hydroxides)-LR (a ~ c) and desorption process (d ~ f). As seen in Fig. 6 **(a ~ c)**, the film-like species coating on the surface of $Cu(OH)_x$-D751, $Cu(OH)_x/Ni(OH)_x$-D751, $Cu(OH)_x/Zn(OH)_x$-D751 resin and it still has obvious porous structured. Compared Fig. 6 **(a ~ c)** with Fig. 2 **(b ~ d)** reveals that a large number of small blocks were dispersedly distributed on the surface of Me(hydroxides)-LR. After the first ammonia desorption, the porous structured on the resin surface was

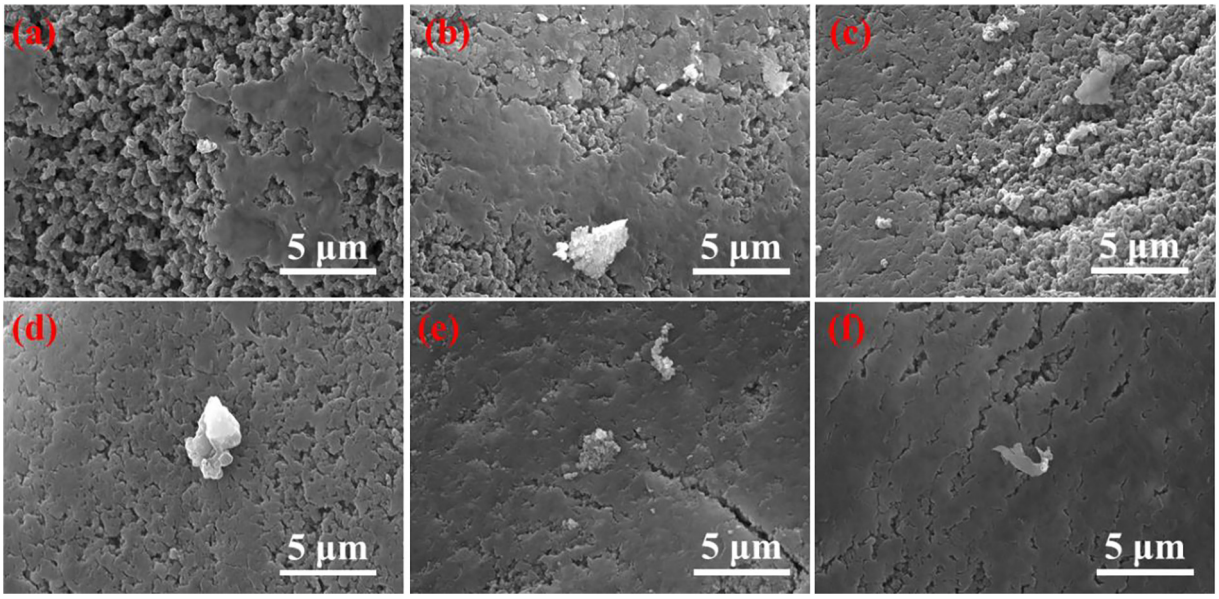

Fig. 6 SEM images of (a) $Cu(OH)_x$-D751, (b) $Cu(OH)_x/Ni(OH)_x$-D751, (c) $Cu(OH)_x/Zn(OH)_x$-D751, (d) $Cu(OH)_x$-D751 after desorption, (e) $Cu(OH)_x/Ni(OH)_x$-D751 after desorption, (f) $Cu(OH)_x/Zn(OH)_x$-D751 after desorption.

reduced, and the distribution of film-like species was more evenly compared Fig. 6 **(d ~ f)** with **(a ~ c).**

As depicted in Fig. S1(b), the N_2 adsorption and desorption isotherms of six resins also shown typical type IV with H1 hysteresis loop. This result was indistinguishable from that in Fig. S1(a). The specific surface area, pore volume and mean pore diameter of the Me(hydroxides)-LR were decreased as compared to Me(ion)-LR due to the reaction between OH^- with metal ion loaded on D751 resin, as shown in Table 4.

The FTIR spectrum of $Cu(OH)_x$-D751, $Cu(OH)_x$/$Ni(OH)_x$-D751, $Cu(OH)_x$/$Zn(OH)_x$-D751 resin are shown in Fig. 3 **(B)**. Compared with Me(ion)-LR (Fig. 4), the –OH stretching vibrations of –COOH groups was shifted from 3453 cm^{-1} to 3449, 3468 to 3448 cm^{-1} and 3475 cm^{-1} to 3451 cm^{-1}, respectively, suggesting that the –OH were participated in the metal hydroxide loading process. The X-ray photoelectron spectroscopy (XPS) measurements were also conducted to further probe the possible ammonia adsorption mechanism onto Me (hydroxides)-LR. The results of XPS spectra of Me (hydroxides)-LR and ammonia saturated Me(hydroxides)-LR are exhibited in Fig. 7 **(A ~ F)**, respectively. As shown in Fig. 7 **(A)**, two main peaks at 934.2 and 953.8 eV can be assigned to Cu $2p_{3/2}$ and Cu $2p_{1/2}$, which were corresponding to $Cu(OH)_x$ and CuO, respectively (Ivanova et al., 2020, Li et al., 2020). And there are two satellite peaks located at 941.0 and 944.0 eV. For the N 1 s region, the peak at 400.0 eV proves the $–NH_2$ groups coming from D751 resin and the peak located at 402.0 eV is attributed to the metal-nitrogen bonds (-N-Cu) coming from the complexation of the $–NH_2$ groups to the Cu ions (Min et al, 2012; Mahata et al, 2021). Furthermore, The O 1 s spectrum of $Cu(OH)_x$-D751 resin is composed of three peaks, with a main peak at 531.5 eV and two short peaks located at 530.5 and 532.6 eV. The peaks at 531.5 and 530.5 eV, which are activated by O atoms in C = O bands (Ou et al, 2006) coming from D751 resin and the -Cu–O bonds (Liang et al, 2018) coming from $Cu(OH)_x$, respectively. Besides, the peak at 532.6 eV, which could be attributed to the absorption of O_2 (Xu et al, 2017). In the case of Ni 2p (Fig. 7(B)) on $Cu(OH)_x$/$Ni(OH)_x$-D751 resin, two main peaks located at 855.9 and 873.8 eV are observed assigned to Ni $2p_{3/2}$ and Ni $2p_{1/2}$ (Álvaro et al, 2019), confirming the existence of $Ni(OH)_x$ and NiO, respectively (Pan et al, 2019). And there are two satellite peaks located at 861.2 and 879.6 eV. In the case of Zn 2p (Fig. 7 (C)) on $Cu(OH)_x$/$Zn(OH)_x$-D751 resin, the binding energies existed at 1022.3 eV is corresponding to $Zn(OH)_x$ (Xie et al, 2020). In addition, after ammonia adsorption, the Cu2p spectrum at Cu $2p_{3/2}$ and Cu $2p_{1/2}$ in $Cu(OH)_x$-D751-NH_3 (Fig. 7 (D)), $Cu(OH)_x$/$Ni(OH)_x$-D751-NH_3 (Fig. 7(E)) and $Cu(OH)_x$/$Zn(OH)_x$-D751-NH_3 (Fig. 7(F)), respectively have a chemical shift toward higher binding energy. And the O1s peak at 530.5 eV was disappeared. Thus, it can be inferred that a coordination exchange has occurred between NH_3 and OH^- on Cu adsorption sites $\overline{(R-Cu(OH)_x)} \rightarrow \overline{(R-Cu(NH_3)_x)}$. Moreover, it can be seen that the Ni2p peak in from Fig. 7(E) shifts 0.3 eV (from 855.9 eV to 856.2 eV) and the Zn2p peak in from Fig. 7(F) shifts 0.4 eV (from 1022.3 eV to 1022.7 eV) to higher binding energy, indicating that a coordination exchange of NH_3 and OH^- on Ni, Zn adsorption sites were also achieved $\overline{(R-Ni(OH)_x} \rightarrow \overline{R-Ni(NH_3)_x}$, $\overline{R-Zn(OH)_x} \rightarrow \overline{R-Zn(NH_3)_x}$.

3.3. Ammonia desorption of Me(hydroxides)-LR

3.3.1. Effect of different desorbents

A static desorption experiment was performed on ammonia-saturated resins using HCl, NaCl, and NaOH as desorbents to investigate the desorption effects of different desorbents, determine the shedding percent of metal ions, and analyze the stability of metal ions in the process of ammonia ligand decomplexation, as shown in Fig. 8 **(a)** and Table 5. The adsorption condition: room temperature (298 ± 2 K), concentration of ammonia solution 100 mg/L, initial pH of solution 11, dosage of NaCl 4 g/L, dosage of resin 6 g/L, stirring speed 120 r/min and reaction time 150 min.

Fig. 8 **(a)** shows that the desorption percent of HCl and NaOH as desorbents was higher than that of NaCl. When the concentration of HCl increased from 0.01 mol/L to 1 mol/L, the desorption percent increased. Combing with Table 5, a large amount of metal ions loaded on the resin dissolution. Using HCl as the desorbent of ammonia-saturated resin, its desorption mechanism is that the NH_3 adsorbed on the resin first reacts with H^+ to convert into NH_4^+ and then dissociates from the coordination with metal ions. To further increase the HCl concentration, the metal ions loaded on the resin were replaced by H^+, which were subsequently released into the solution, causing heavy metal pollution. Moreover, the desorption percent and metal ion shedding percent of NaOH as desorbent were slightly lower than those of HCl. Using NaOH as the desorbent of ammonia-saturated resin ($\overline{R-Me(NH_3)_n(OH)_m}$), it reduces the stability of $\overline{R-Me(NH_3)_n(OH)_m}$, which promotes the shift of

Table 4 N_2 adsorption–desorption analysis data of Me(hydroxides)-LR.

Different types of Me(hydroxides)-LR	State of Me(hydroxides)-LR	Surface area (m^2/g)	Pore volume (cm^3/g)	Mean pore diameter (nm)
$Cu(OH)_x$-D751	Unused	12.2	0.013	4.37
	After first adsorption	12.9	0.014	4.47
	After first desorption	12.0	0.013	4.40
$Cu(OH)_x$/$Ni(OH)_x$-D751	Unused	15.2	0.016	4.28
	After first adsorption	14.5	0.016	4.34
	After first desorption	14.5	0.016	4.31
$Cu(OH)_x$/$Zn(OH)_x$-D751	Unused	15.3	0.016	4.29
	After first adsorption	14.0	0.015	4.32
	After first desorption	14.2	0.015	4.35

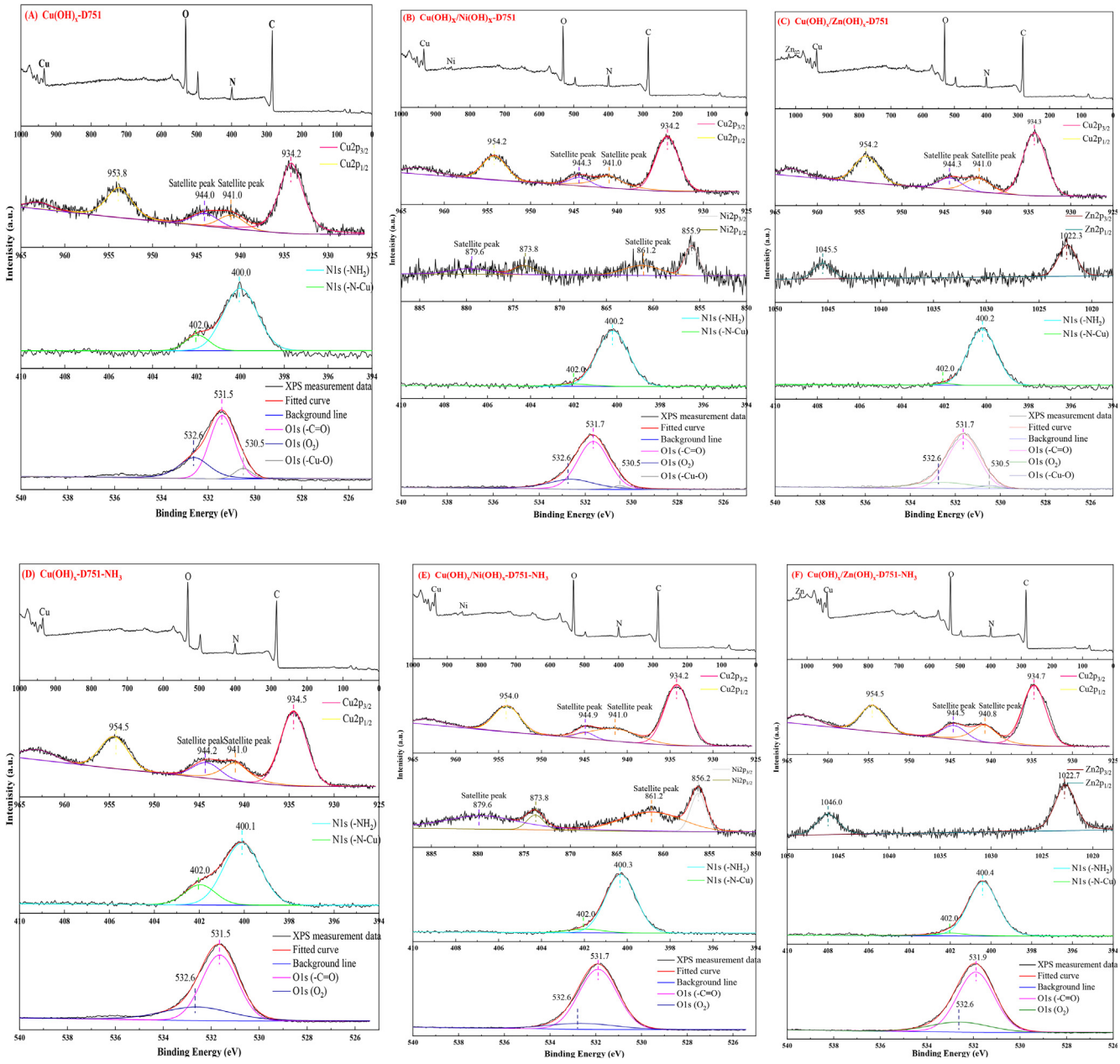

Fig. 7 XPS spectra of Me(hydroxides)-LR before and after ammonia adsorption (A) $Cu(OH)_x$-D751 (B) $Cu(OH)_x/Ni(OH)_x$-D751, (C) $Cu(OH)_x/Zn(OH)_x$-D751, (D) $Cu(OH)_x$-D751-NH_3, (E) $Cu(OH)_x/Ni(OH)_x$-D751-NH_3, (F) $Cu(OH)_x/Zn(OH)_x$-D751-NH_3.

$\overline{R-Me(NH_3)_n(OH)_m}$ into $R-Me(OH)_x$ and then NH_3 be eluted from the resin. In addition, when the concentration of NaOH increased to 1 mol/L, the resin appears to blacken according to naked eye observation (**Fig.S3**), which probably caused by combination of the Me(hydroxides)-LR and excessive OH^- to form black CuO_x ($\overline{R-Cu(OH)_x} \rightarrow \overline{R-CuOx}$). Meanwhile, as can be seen from the data in Table 5, the phenomenon of metal ion shedding is still obvious. When 1 mol/L NaCl solution was used as a neutral salt for the desorption of ammonia-saturated Me(ion)-LR, the ammonia desorption percent of $Cu(OH)_x$-D751, $Cu(OH)_x/Ni(OH)_x$-D751 and $Cu(OH)_x/Zn(OH)_x$-D751 resins were 67%, 64%, 70%, respectively. The ammonia desorption percent of NaCl as desorbent is lower than that of the other two desorbents, but those resins maintained good stability and low metal shedding percent.

3.3.2. Effect of NaCl concentration

The desorption experiment was conducted on ammonia-saturated adsorbents ($Cu(OH)_x$-D751-NH_3, $Cu(OH)_x/Ni(OH)_x$-D751-NH_3 and $Cu(OH)_x/Zn(OH)_x$-D751-NH_3 resins) using NaCl as desorbents to investigate the influence of NaCl concentration on ammonia desorption. The results can be seen from Fig. 8(b) that the ammonia desorption percent increased with the increasing of NaCl concentration. When NaCl concentration was 1.5 mol/L (87.66 g/L), the maximum desorption percent of $Cu(OH)_x$-D751 resin for ammonia was 67.29%. For

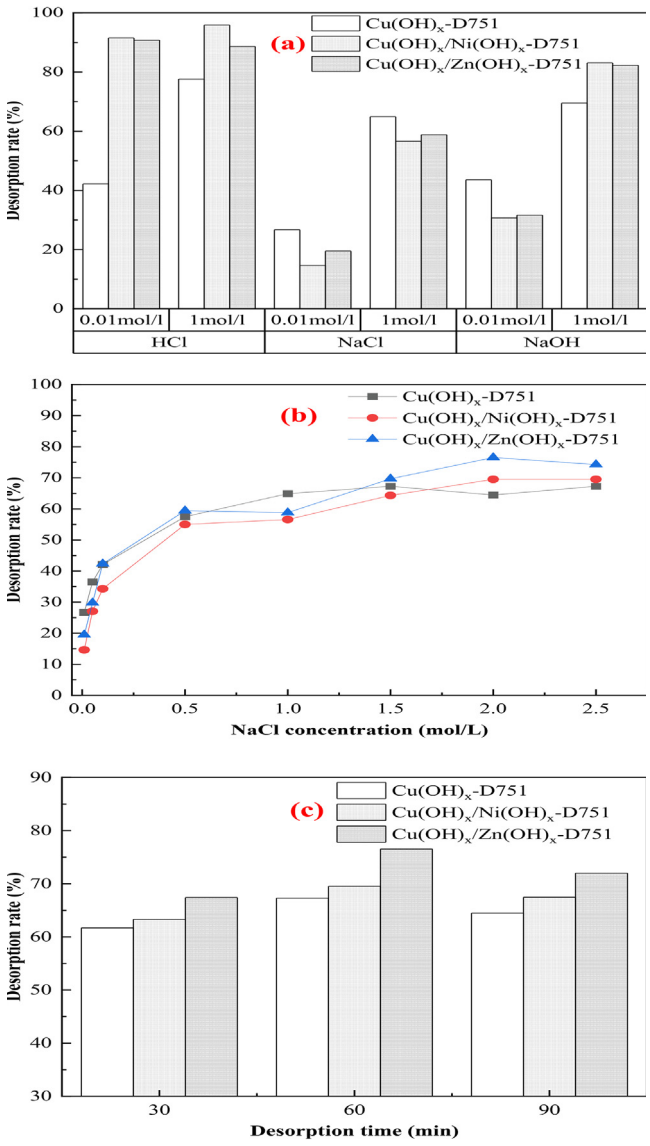

Fig. 8 The ammonia desorption effects of (a) different desorbents, (b) NaCl concentration, (c) desorption time.

$Cu(OH)_x/Ni(OH)_x$-D751 and $Cu(OH)_x/Zn(OH)_x$-D751 resin, the maximum desorption percents were 69.53%, 76.54% when the NaCl concentration was 2 mol/L (116.88 g/L). The concentration of NaCl solution as desorbents was much higher than the initial concentration of NaCl in the reaction solution (4 g/L), indicating that the Me(hydroxides)-LR has a good stability and is suitable for the treatment of ammonia wastewater containing high salinity.

3.3.3. *Effect of desorption time*

In this experiment, the ammonia-saturated $Cu(OH)_x$-D751 resin (0.6 g) was soaked in 100 mL 1.5 mol/L NaCl solution and $Cu(OH)_x/Ni(OH)_x$-D751 and $Cu(OH)_x/Zn(OH)_x$-D751 resins (0.6 g) were soaked in 100 mL 2.0 mol/L NaCl solution, respectively, under shaking at 120 r/min for desired time (30 min, 60 min, 90 min). The results presented in Fig. 8(c) shows that the desorption percent of Cu(OH)x-D751, Cu(OH)x/Ni(OH)x-D751 and Cu(OH)x/Zn(OH)x-D751 resin for ammonia in solution increased firstly and then decreased with the increasing of desorption time, and the maximum desorption percent of three resins reached the maximum at 60 min, which were 67.29%, 69.53% and 76.54%, respectively. A probably reason is that when NaCl solution is used as desorbent for the desorption of ammonia-saturated resin, the maximum transition from $\overline{R-Me(NH_3)_n(OH)_m}$ into $\overline{R-Me(OH)_x}$ is achieved, and then NH_3 be eluted from the resin. And further prolonging the desorption time, the desorbed ammonia was re-adsorbed on the resin.

3.4. *The adsorption pathway for ammonia in solution in the metal ion/metal hydroxide loaded resin*

According to the above experimental and characterization results, the adsorption pathway for ammonia in solution in the metal ion/metal hydroxide loaded resin can be inferred, taking Cu^{2+}-D751 and $Cu(OH)_x$-D751 resins as example, as shown in Fig. 9. Under alkaline conditions (pH = 11), ammonia mainly exists in a free state (NH_3(aq)). The adsorption sites on metal ion loaded resin (Me(ion)-LR) and metal hydroxide loaded resin (Me(hydroxide)-LR) absorbed portion of OH^- in solution to make the resin surface showed electronegative, which was conducive to the adsorption of NH_4^+ in the form of ionic bonds through electrostatic interaction. On the other hand, the metal adsorption sites on Me(ion)-LR and Me(hydroxide)-LR resin form a coordination bond with N atom in NH_3 by sharing the lone pair of electrons provided by N, O atom, thus forming a metal ammonia complex loaded resin. In summary, the ammonia removal by metal ion/metal hydroxide loaded resin was primarily attributable to coordination complexation and electrostatic interaction.

Table 5 Effect of different desorbents on stability of Me(hydroxides)-LR.

Concentration of desorbents (mol/L)	Metal ion	NaOH		HCl		NaCl	
	/	0.01	1.0	0.01	1.0	0.01	1.0
$Cu(OH)_x$-D751 shedding percent (%)	Cu(Ⅱ)	0.04	3.37	0.06	84.62	ND	0.06
$Cu(OH)_x/Ni(OH)_x$-D751 shedding percent (%)	Cu(Ⅱ)	0.02	1.12	0.99	81.57	ND	0.03
	Ni(Ⅱ)	ND	1.59	3.29	22.69	0.10	4.81
$Cu(OH)_x/Zn(OH)_x$-D751shedding percent (%)	Cu(Ⅱ)	ND	2.56	0.77	95.76	0.02	0.02
	Zn(Ⅱ)	1.35	25.52	4.71	45.15	ND	0.71

ND: the concentration of metal ions in solution was not detected by the atomic absorption spectroscopy.

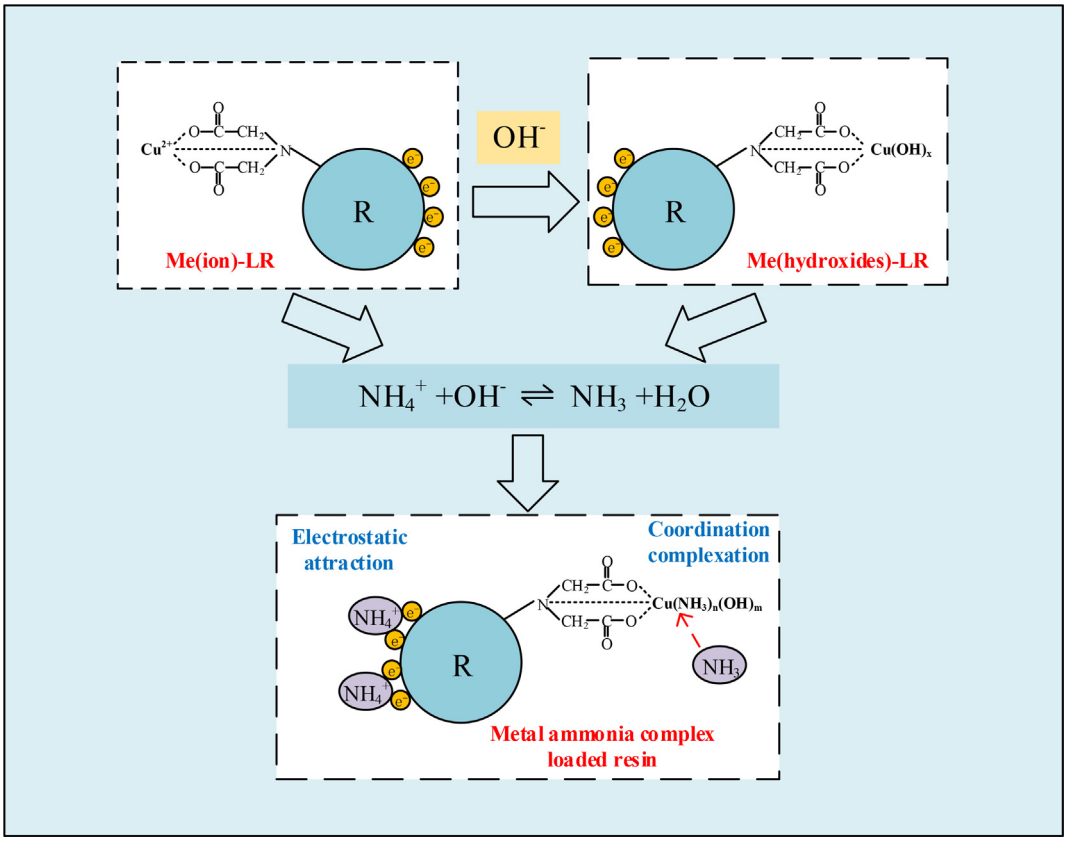

Fig. 9 The adsorption pathway for ammonia in solution in the metal ion/metal hydroxide loaded resin.

4. Conclusion

In order to improve the stability of metal ions on the Me(ion)-LR during ammonia ligand decomplexation, a novel Me(hydroxides)-LR was prepared to efficiently remove ammonia from solutions containing high salinity. Based on the results of this study, we draw the following conclusions.

1). the optimal ammonia adsorption capacity was obtained by using $Cu(OH)_x$-D751, $Cu(OH)_x/Ni(OH)_x$-D751 and $Cu(OH)_x/Zn(OH)_x$-D751 resin prepared under the conditions of NaOH concentration 0.005, 0.01, 0.01 mol/L, respectively and the modification time 15 min.

2). the stability of metal ion during ammonia ligand decomplexation could be improved by NaOH modification.

3). the ammonia desorption percent of Me(hydroxides)-LR with NaCl solution as desorbent was lower than that of the other two desorbents (HCl and NaOH), but resins maintained better stability and lower metal shedding percent. The corresponding maximum desorption percent of $Cu(OH)_x$-D751, $Cu(OH)_x/Ni(OH)_x$-D751 and $Cu(OH)_x/Zn(OH)_x$-D751 resin for ammonia was 67.29%, 69.53% and 76.54%, respectively under the condition of the NaCl as desorbent, NaCl concentration 1.5, 2, 2 mol/L, respectively and the desorption time 60 min.

4). the ammonia removal by Me(hydroxides)-LR was primarily attributable to coordination complexation and electrostatic interaction.

Ethical approval

This work has not been published before and not under consideration for publication anywhere else.

6. Consent to participate

This publication has been approved by all co-authors.

7. Consent to publish

This publication has been approved by all co-authors.

Funding

This work was supported by the National Natural Science Foundation of China (grant number 51864021), and the authors are grateful for the helpful suggestions and evaluations given by many anonymous reviewers.

9. Available of data and materials

Authors agree to store the data and materials of the research results in a common repository.

CRediT authorship contribution statement

Chen Liu: Formal analysis, Investigation, Validation, Writing – original draft. **Tingsheng Qiu:** Formal analysis, Investigation, Methodology, Resources. **Yunnen Chen:** Conceptualization, Formal analysis, Investigation, Funding acquisition, Writing – review & editing.

Declaration of Competing Interest

The authors declare that they have no known competing financial interests or personal relationships that could have appeared to influence the work reported in this paper.

Appendix A. Supplementary material

Supplementary data to this article can be found online at https://doi.org/10.1016/j.arabjc.2023.104879.

References

AtkinsJr, P.F., Scherger, D.A., 2013. A review of physical chemical methods for nitrogen removal from wastewaters. Prog. Wat. Tech. 8, 713–719. https://doi.org/10.1016/B978-1-4832-1344-6.50051-4.

Álvaro, A., Carlos, G., Martha, N.G., Fernando, M.O., 2019. XPS fitting model proposed to the study of Ni and La in deactivated FCC catalysts. J. Electron. Spectrosc. 233, 5–10. https://doi.org/10.1016/j.elspec.2019.03.007.

Al-Sheikh, F., Moralejo, C., Pritzker, M., Anderson, W.A., Elkamel, A., 2021. Batch adsorption study of ammonia removal from synthetic/real wastewater using ion exchange resins and zeolites. Sep. Sci. Technol. 56 (3), 462–473. https://doi.org/10.1080/01496395.2020.1718706.

Berrin, T., 2012. Significance of thermodynamic and physical characteristics on permeation of ions during membrane separation: hydrated radius, hydration free energy and viscous effects. Sep. Purif. Technol. 86, 119–126. https://doi.org/10.1016/j.seppur.2011.10.033.

Clark, B., Tarpeh, W.A., 2020. Selective recovery of ammonia nitrogen from wastewaters with transition metal-loaded polymeric cation exchange adsorbents. Chem. Eur. J. 26 (44), 10099–10112. https://doi.org/10.1002/chem.202002170.

Chen, Q.Z., Zhou, K.G., Chen, Y., Wang, A.H., Liu, F., 2017. Removal of ammonia from aqueous solutions by ligand exchange onto a Cu(II)-loaded chelating resin: kinetics, equilibrium and thermodynamics. RSC Adv. 7, 12812. https://doi.org/10.1039/c6ra28287c.

Chen, Y., Wu, Y., Liu, C., Guo, L., Nie, J., Chen, Y., Qiu, T., 2018. Low-temperature conversion of ammonia to nitrogen in water with ozone over composite metal oxide catalyst. J. Environ. Sci.-China 66, 265–273. https://doi.org/10.1016/j.jes.2017.04.032.

Dong, S.X., Wang, Y.L., Zhao, Y.W., Zhou, X.H., Zheng, H.L., 2017. La^{3+}/$La(OH)_3$ loaded magnetic cationic hydrogel composites for phosphate removal: effect of lanthanum species and mechanistic study. Water Res. 126 (1), 433–441. https://doi.org/10.1016/j.watres.2017.09.050.

El-Bayaa, A.A., Badawy, N.A., AlKhalik, E.A., 2009. Effect of ionic strength on the adsorption of copper and chromium ions by vermiculite pure clay mineral. J. Hazard. Mater. 170 (2–3), 1204–1209. https://doi.org/10.1016/j. jhazmat.2009.05.100.

Epsztein, R., Shaulsky, E., Qin, M., Elimelech, M., 2019. Activation behavior for ion permeation in ion-exchange membranes: role of ion dehydration in selective transport. J. Membr. Sci. 580, 316–326. https://doi.org/10.1016/j.memsci.2019.02.009.

Fu, Q., Zheng, B., Zhao, X., Wang, L., Liu, C., 2012. Ammonia pollution characteristics of centralized drinking water sources in China. J. Environ. Sci. 24 (10), 1739–1743. https://doi.org/10.1016/S1001-0742(11)61011-5.

Helfferich, F., 1962. Ligand exchange. I. equilibria. J. Am. Chem. Soc. 84 (17), 3237–3242. https://doi.org/10.1021/ja00876a003.

Huang, H.M., Xiao, X.M., Yan, B., Yang, L.P., 2010. Ammonium removal from aqueous solutions by using natural Chinese (Chende) zeolite as adsorbent. J. Hazard. Mater. 175 (1–3), 247–252. https://doi.org/10.1016/j.jhazmat.2009.09.156.

Huang, J., Kankanamge, N.R., Chow, C., Welsh, D.T., Li, T., Teasdale, P.R., 2018. Removing ammonium from water and wastewater using cost-effective adsorbents: a review. J. Environ. Sci. 63, 174–197. https://doi.org/10.1016/j.jes.2017.09.009.

Igberase, E., Osifo, P., Ofomaja, A., 2017. The adsorption of Pb, Zn, Cu, Ni, and Cd by modified ligand in a single component aqueous solution: equilibrium, kinetic, thermodynamic, and desorption studies. Int. J. Anal. Chem 1–15. https://doi.org/10.1155/2017/6150209.

Ivanova, T.M., Maslakov, K.I., Sidorov, A.A., Kiskin, M.A., Linko, R.V., Savilov, S.V., Lunin, V.V., Eremenko, I.L., 2020. XPS detection of unusual Cu(II) to Cu(I) transition on the surface of complexes with redox-active ligands. J. Elect. Spectrosc. 238, 1–5. https://doi.org/10.1016/j.elspec.2019.06.010.

Jiang, J., Xu, R.K., Li, S.Z., 2010. Effect of ionic strength and mechanism of Cu(II) adsorption by goethite and γ-Al_2O_3. J. Chem. Eng. Data 55 (12), 5547–5552. https://doi.org/10.1021/je100271u.

Keyikogluab, R., Karatasab, O., Rezaniac, H., Kobyaad, M., Vatanpourc, V., Khataeeae, A., 2021. A review on treatment of membrane concentrates generated from landfill leachate treatment processes. Sep. Purif. Technol. 259, (25). https://doi.org/10.1016/j.seppur.2020.118182 118182.

Koon, J.H., Kaufman, W.J., 1975. Ammonia removal from municipal wastewaters by ion exchange. J. (Water Pollut. Control Fed.) 47 (3), 448–465. https://doi.org/10.2307/25038654.

Lahav, O., Asher, R.B., Gendel, Y., 2015. Potential applications of indirect electrochemical ammonia oxidation within the operation of freshwater and saline-water recirculating aquaculture systems. Aquacult. Eng. 65, 55–64. https://doi.org/10.1016/j.aquaeng.2014.10.009.

Lefebvre, O., Moletta, R., 2006. Treatment of organic pollution in industrial saline wastewater: a literature review. Water Res. 40 (20), 3671–3682. https://doi.org/10.1016/j.watres.2006.08.027.

Leyva-Ramos, R., Monsivais-Rocha, J.E., Aragon-Pia, A., Berber-Mendoza, M.S., Guerrero-Coronado, R.M., Alonso-Davila, P., Mendoza-Barron, J., 2010. Removal of ammonium from aqueous solution by ion exchange on natural and modified chabazite. J. Environ. Manage. 91 (12), 2662–2668. https://doi.org/10.1016/j.jenvman.2010.07.035.

Li, H.B., Xie, F.Z., Zhang, K.H., Li, G.L., Chen, Q.D., Dong, W.W., Cheng, C., Liu, Q., 2020. Mechanism of Cu(Ⅱ) adsorption by D311 resin under acidic conditions. Polym. Mater. Sci. Eng. 36 (06). https://doi.org/10.16865/j.cnki.1000-7555.2020.0136.

Li, J., Bai, L., Qiang, Z., Dong, H., Wang, D., 2018. Nitrogen removal through "Candidatus Brocadia sinica" treating high-salinity and low-temperature wastewater with glycine addition: Enhanced performance and kinetics. Bioresour. Technol. 270 (1), 755–761. https://doi.org/10.1016/j.biortech.2018.09.101.

Liu, M., Peng, Y.Z., Wang, S.Y., Liu, T.T., Xiao, H., 2014. Enhancement of anammox activity by addition of compatible solutes at high salinity conditions. Bioresour. Technol. 167, 560–563. https://doi.org/10.1016/j.biortech.2014.06.015.

Liang, H.Y., Lin, J.H., Jia, H.N., Chen, S.L., Qi, J.L., Cao, J., Lin, T. S., Fei, W.D., Feng, J.C., 2018. Hierarchical NiCo-LDH@NiOOH core-shell heterostructure on carbon fiber cloth as battery-like electrode for supercapacitor. J. Power Sources 378, 248–254. https://doi.org/10.1016/j.jpowsour.2017.12.046.

Min, H., Girard-Lauriault, P.L., Gross, T., Lippitz, A., Dietrich, P., Unger, W.E.S., 2012. Ambient-ageing processes in amine self-assembled monolayers on microarray slides as studied by ToF-SIMS with principal component analysis, XPS, and NEXAFS spectroscopy. Anal. Bioanal. Chem. 403 (2), 613–623. https://doi.org/10.1007/s00216-012-5862-5.

Mahata, B.K., Chung, K., Chang, S., 2021. Removal of ammonium nitrogen (NH_4^+-N) by Cu-loaded amino-functionalized adsorbents. Chem. Eng. J. 411, (7). https://doi.org/10.1016/j.cej.2021.128589 128589.

Mohd, R.A., Mohd, H.D.O., Rozaimi, A.S., Mohd, H.P., Ismail, A. F., Azeman, M., Mukhlis, A.R., Juhana, J., 2019. Current trends and future prospects of ammonia removal in wastewater: a comprehensive review on adsorptive membrane development. Sep. Purif. Technol. 213 (114–132), 114–132. https://doi.org/10.1016/j.seppur.2018.12.030.

Nawrocki, J., Rigney, M., Mccormick, A., Carr, P.W., 1993. Chemistry of zirconia and its use in chromatography. J. Chromatogr. A 657, 229–282. https://doi.org/10.1016/0021-9673(93)80284-F.

Ou, G.P., Song, Z., Gui, W.M., Zhang, F.J., 2006. Analysis of PTCDA/ITO surface and interface using X-ray photoelectron spectroscopy and atomic force microscopy. Chinese J. Semicond. 27 (2), 229–234. https://doi.org/10.3321/j.issn:0253-4177.2006.02.006.

Prabhu, S.M., Meenakshi, S., 2014. Effect of metal ions loaded onto iminodiacetic acid functionalized cation exchange resin for selective fluoride removal. Desalin. Water Treat. 52, 2527–2536. https://doi.org/10.1080/19443994.2013.792747.

Pan, Y., Hu, G., Lu, J., Xiao, L., Zhuang, L., 2019. $Ni(OH)_2$-Ni/C for hydrogen oxidation reaction in alkaline media. J. Energy Chem. 29, 111–115. https://doi.org/10.1016/j.jechem.2018.02.011.

Qin, W.W., Yang, Z.F., Hou, Q.Y., Cao, T.N., 2011. Health risk assessment of drinking water in poyang lake region in Jiangxi Province. Geoscience 25 (01), 182–188. https://doi.org/10.3724/SP.J.1077.2011.00311.

Rahman, M.M., Salleh, M.A.M., Rashid, U., Ahsan, A., Hossain, M. M., Ra, C.S., 2014. Production of slow release crystal fertilizer from wastewaters through struvite crystallization-a review. Arab. J. Chem. 7, 139–155.

Saha, D., Deng, S., 2010. Adsorption equilibrium and kinetics of CO_2, CH_4, N_2O, and NH_3 on ordered mesoporous carbon. J. Colloid Interface Sci. 345, 402–409. https://doi.org/10.1016/j.jcis.2010.01.076.

Sengupta, A.K., Zhu, Y., Hauze, D., 1991. Metal(II) ion binding onto chelating exchangers with nitrogen donor atoms: some new observations and related implications. Environ. Sci. Technol. 25 (3), 481–488. https://doi.org/10.1021/es00015a016.

Wang, Z., Luo, G., Li, J., Chen, S.Y., Li, Y., Li, W.T., Li, A.M., 2016. Response of performance and ammonia oxidizing bacteria community to high salinity stress in membrane bioreactor with elevated ammonia loading. Bioresour. Technol. 216 (1), 714–721. https://doi.org/10.1016/j.biortech.2016.05.123.

Wu, Y., 2017. Study on preparation of resin modified by metal ions and its application in dealing with high salt and ammonia from the the rare-earth wastewater. Jiangxi Univ. Sci. Technol., Ganzhou, Jiangxi, China 29–39. https://doi.org/10.7666/d.D01423882.

Xu, P., Miao, C., Feng, J., Cheng, K., Ye, K., Yin, J., Cao, D., Wang, G., Cai, Z., Li, Q., 2017. A novel material NiOOH directly grown on in-situ etched $Cu(OH)_2$ nanowire with high performance of electrochemical energy storage. Electrochim. Acta 232, 445–455. https://doi.org/10.1016/j.electacta.2017.02.158.

Xie, X., Tong, X., Zhang, S.D., Kang, B.W., Li, J., 2020. Mechanism of ammonium chloride strengthen sphalerite's activation by copper under low alkaline condition. Metal. Mine. 2, 1–8. https://doi.org/10.19614/j.cnki.jsks.202002001.

Yu, R., Yu, X., Fu, J., Zhang, Y., Liu, Y., Zhang, Y., Wu, S., 2021. Removal of ammonia nitrogen in aquaculture wastewater by composite photocatalyst TiO_2/carbon fibre. Water Environ. J. 35 (3), 962–970. https://doi.org/10.1111/wej.12686.

Yuan, W.Z., Mao, P., Yu, Q.M., Tang, B.Z., Zheng, Q., 2006. Synthesis and characterization of polystyrene/nanosilica organic-inorganic hybrid. Chem. Res. Chin. Univ. 22, 797–802. https://doi.org/10.1016/S1005-9040(06)60215-8.

Zhang, H., Dou, H.Y., Tao, Z.Y., 1990. The sorption behavious of UO_2^{2+}, Cu^{2+}, Ni^{2+}, Zn^{2+} and Co^{2+} on the macroporous chelating ion exchange resin D751. J. Nucl. Radiochem. 12 (4), 214. https://doi.org/10.1007/BF02006102.

Zhang, L., Xu, E.G., Li, Y., Liu, H., Vidal-Dorsch, D.E., Giesy, J.P., 2018. Ecological risks posed by ammonia nitrogen (AN) and unionized ammonia (NH_3) in seven major river systems of China. Chemosphere 202 (1), 36–44. https://doi.org/10.1016/j.chemosphere.2018.03.098.

Zhou, K., Chen, Q., Jiang, K., Hu, Y,J., Peng, J. L., 2015. Ammonia-nitrogen desorption and circulating adsorption ability of copper loaded chelating resin. J Cent South Univ, 46(11), 3999-4004. https://doi.org/10.11817/j.issn.1672-7207.2015.11.004

Zhu, L., Dong, D.M., Hua, X.Y., Guo, Z.Y., Liang, D.P., 2016. Ammonia nitrogen removal from acetylene purification wastewater from a PVC plant by struvite precipitation. Water. Sci. Technol. 74 (2), 508–515. https://doi.org/10.2166/wst.2016.239.

Zhang, X.T., Ma, C.H., Wen, K., Han, R.P., 2020. Adsorption of phosphate from aqueous solution by lanthanum modified macroporous chelating resin. Korean J. Chem. Eng. 37 (5), 766–775. https://doi.org/10.1007/s11814-020-0495-4.